A pyrene-appended spiropyran for selective photo-switchable binding of Zn(II): UV-visible and fluorescence spectroscopy studies of binding and non-covalent attachment to graphene, graphene oxide and carbon nanotubes.

A. Perry,*[a] S.J. Green,[b] D.W. Horsell,[b] S.M. Hornett[b] and M.E. Wood[a]

a. Biosciences, College of Life and Environmental Science, University of Exeter, Geoffrey Pope Building, Exeter EX4 4QD, UK

b. Department of Physics, College of Engineering, Mathematics and Physical Sciences, University of Exeter, Stocker Road, Exeter EX4 4QL, UK.

Abstract

Synthesis of photo-switchable, Zn^{2+} sensitive hybrid materials was achieved by facile non-covalent functionalization of graphene, graphene oxide and carbon nanotubes with a pyrene-appended spiropyran. Solution phase binding studies, using UV-visible and fluorescence spectroscopy, indicated that the pyrene-spiropyran dyad was highly selective for Zn^{2+} over a range of potentially competitive cations and that binding occurred with 1:1 stoichiometry and a binding constant of $K = 1.4 \times 10^4$ mol^{-1} dm^3 at 295 K. Zn^{2+} binding was promoted by UV irradiation or in darkness and reversed upon irradiation with visible light.

1. Introduction

2

A spiropyran (a spiro-fused chromene-indoline (e.g. **1**, Scheme 1)) is a photochromic molecule that under UV illumination switches to its structural isomer merocyanine (e.g. **2**), with the reverse process promoted by visible light (or heat) (e.g. Scheme 1).[1]

1; spiropyran form   **2**; merocyanine form
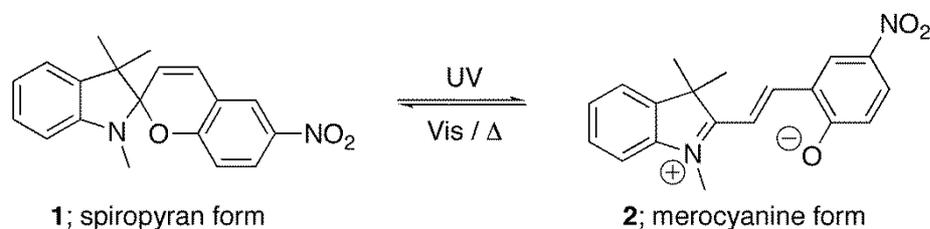
Scheme 1 – Spiropyran–merocyanine equilibrium

The uncharged spiropyran and the zwitterionic merocyanine have markedly different physical and optical properties, which has led to much research into their use in producing dynamic materials.[2] For example, spiropyrans have been attached to carbon nanotubes both by covalent[3] and non-covalent[4] means, the latter predominantly by linking the spiropyran to a pyrene and using π-π stacking between the pyrene and nanotube as anchorage. The usual aim of these studies is to utilise the large difference in dipole moment between the spiropyran and the merocyanine to confer light-addressable switching of the electronic and/or optical properties of the nanotube.[3,4] For this purpose, non-covalent modification appears to be preferable to covalent modification, in that it does not unduly disrupt the carbon framework.[5] Pyrene-appended spiropyrans (e.g. **3**, Figure 1) have been non-covalently attached to graphene and shown to confer reversible optical modification of the Dirac point[5] and the theoretical aspects of the spiropyran-nanotube[6] and the spiropyran-graphene[7] interaction have been considered.
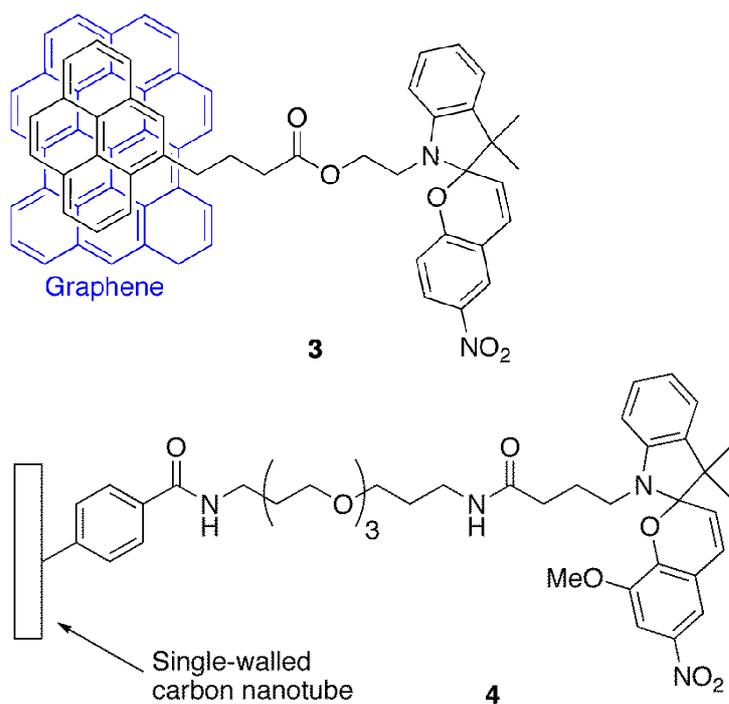
*Figure 1 – Covalent and non-covalent attachment of spiropyrans **3** and **4** to graphene and carbon nanotubes*

Departing somewhat from the usual rationale of a light-addressable switch, Del Canto et al.[8] looked to create a carbon-nanotube-borne, photo-releasing Zn^{2+} drug-delivery system from spiropyran-modified carbon nanotubes (**4**, Figure 1). Their methodology used amide coupling to link a polyethylene glycol moiety appended to the indolic nitrogen of spiropyran, to single-walled carbon nanotubes pre-functionalized (using diazonium-salt chemistry) with benzoic acid groups. The benzopyran unit of the spiropyran was modified with a methoxy group in the 8′ position such that binding of the Zn^{2+} occurred in the merocyanine form, bridging between the methoxy oxygen and the negatively charged phenolate ion, with additional stabilisation of the complex provided by the insertion of an electron-withdrawing nitro group in the benzopyran 6' position. The binding was light-reversible (binding in the dark, releasing in visible light) in a mixed solvent of dichlorobenzene and acetonitrile, plus it was possible to produce a suspension of the material in water.

5; R =

6; R =
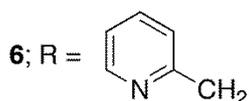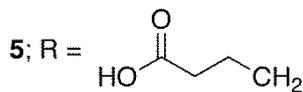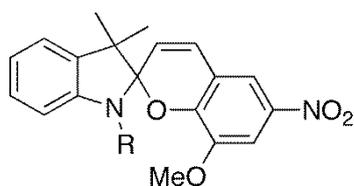
Figure 2 – Zn(II)-binding spiropyrans

In previous studies[9,10] the same group have synthesised analogous light-reversible, Zn^{2+}-binding spiropyrans without attachment to any support, in one case[9] with a butanoic acid side chain appended to the indolic nitrogen (Figure 2, **5**) – giving a 2:1 spiropyran-to-zinc complex stoichiometry in acetonitrile (with possible involvement of the carboxylic acid in the binding interaction) – and in a further case[10] with functionalization of the indolic nitrogen with a methyl pyridine moiety (Figure 2, **6**), such that chelation of the Zn^{2+} (now in 1:1 stoichiometry in acetonitrile) could occur between the pyridine nitrogen lone pair, the phenolate anion and the oxygen of the methoxy group (Figure 3). Compound **5** proved unselective amongst M^{2+} cations, whereas **6**, studied by UV-visible, fluorescence and ^{1}H NMR spectroscopy, showed Zn^{2+} selectivity over a range of possibly competing ions in acetonitrile and was thus viewed as a potential sensing label for Zn^{2+} in a biological and environmental context, though no measurements were made in aqueous media.

5

MC-6:Zn²⁺ complex
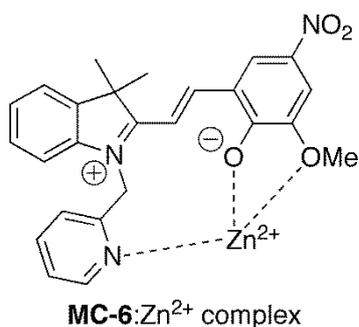
*Figure 3 – Proposed[10] tridentate binding of the merocyanine isomer of **6** with Zn²⁺*

An attractive proposition is to produce a pyrene-appended analogue **7** (Figure 4) of the

pyridine-containing spiropyran **6**. Firstly, in solution, the pyrene itself is a second fluorescent

label for Zn^{2+} in addition to the spiropyran itself and, secondly, it permits simple, non-

covalent attachment to carbon-based materials – in particular, to graphene, graphene oxide

and carbon nanotubes. As noted above, spiropyran-pyrene dyads have previously been used

for non-covalent derivatisation of carbon nanotubes and graphene;[4,5] however, this has yet to

be exploited with respect to spiropyran-based cation receptors. Furthermore, graphene oxide

has not, to the authors' knowledge, been non-covalently modified with spiropyran using

pyrene anchor groups (it has been non-covalently modified by self-assembly of a silyl-

appended spiropyran[11] for the purposes of detecting fluoride in aqueous media).

6
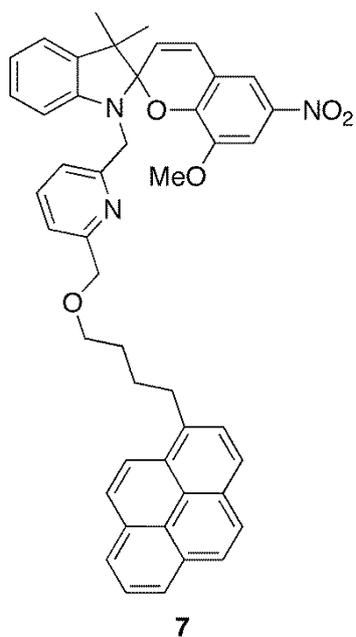
Figure 4 – Proposed Zn²⁺ binding spiropyran with ether-linked pyrene anchor group

In the work presented here, a pyrene-appended Zn^{2+}-binding spiropyran **7** has been synthesised. This material is shown by UV-visible and fluorescent spectroscopy to bind Zn^{2+} selectively and light-reversibly in a wide range of solvents and also to attach non-covalently to graphene oxide, graphene and carbon nanotubes. The latter two hybrid materials display retention of the Zn^{2+}-binding action and so provide new carbon-based platforms for sensing and switching applications.

7

2. Results and Discussion

2.1. Synthesis of spiropyran-pyrene dyad 7

7 was synthesised from commercially available starting materials in three steps (Scheme 2).

Treatment of 1-pyrenebutanol (**8**) and bis(bromomethyl)pyridine (**9**; 2 eq.) with sodium

hydride in refluxing THF gave the ether **10** in 61% yield. *N*-Alkylation of 2,3,3-

trimethylindolenine (**11**) with **10** was sluggish and highly sensitive to reaction stoichiometry.

Optimal conditions required exposure of **10** (1 eq.) to 2,3,3-trimethylindolenine (1.7 eq.) in

the presence of excess potassium carbonate under acetonitrile reflux for 40 h. The indolium

salt intermediate was not isolated; rather, base-mediated rearrangement occurred in-situ to

give the enamine **12**. **12** was sensitive to silica gel chromatography, hence condensation with

3-methoxy-5-nitrosalicylaldehyde (**13**) was performed on crude material to give the target

spiropyran–pyrene dyad **7** in 11% overall yield.
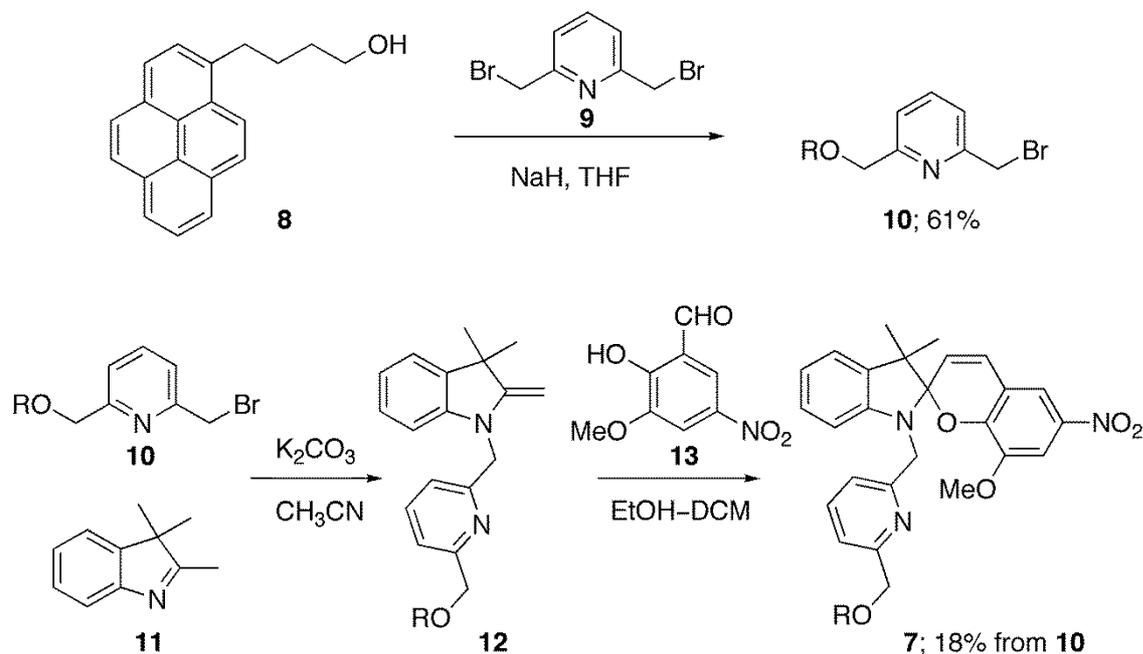
Scheme 2 – Synthesis of spiropyran 7. R = Pyrenebutyl.

2.2. Binding studies of 7 with metal cations

2.2.1. Zn^{2+} selectivity of 7

Initial experiments employed UV-visible spectroscopy to assess the metal cation binding

behaviour of **7**. Addition of 2.5 eq. $Zn(NO_3)_2.5H_2O$ to a 0.1 mM solution of **7** in acetonitrile,

followed by white light irradiation, gave a colourless solution which displayed limited visible

absorbance (Figure 5). After 5 minutes in the dark, the same solution became orange and

showed a strong absorbance at 485 nm, consistent with merocyanine formation and

concomitant metal chelation. A stable equilibrium was attained after 30 minutes. UV

irradiation (366 nm) of a similar solution of **7** and $Zn(NO_3)_2.5H_2O$ in acetonitrile promoted

more rapid merocyanine formation, requiring under 15 minutes to establish a similar

merocyanine concentration to that observed under darkness. Exposure of this solution to

several light-dark cycles gave reproducible and persistent photochromic behaviour (Figure 6).

In contrast, in the absence of Zn^{2+}, a solution of 0.1 mM of **7** in acetonitrile containing no

Zn^{2+} remained colourless, regardless of darkness, UV or white light irradiation (Figure 5b).
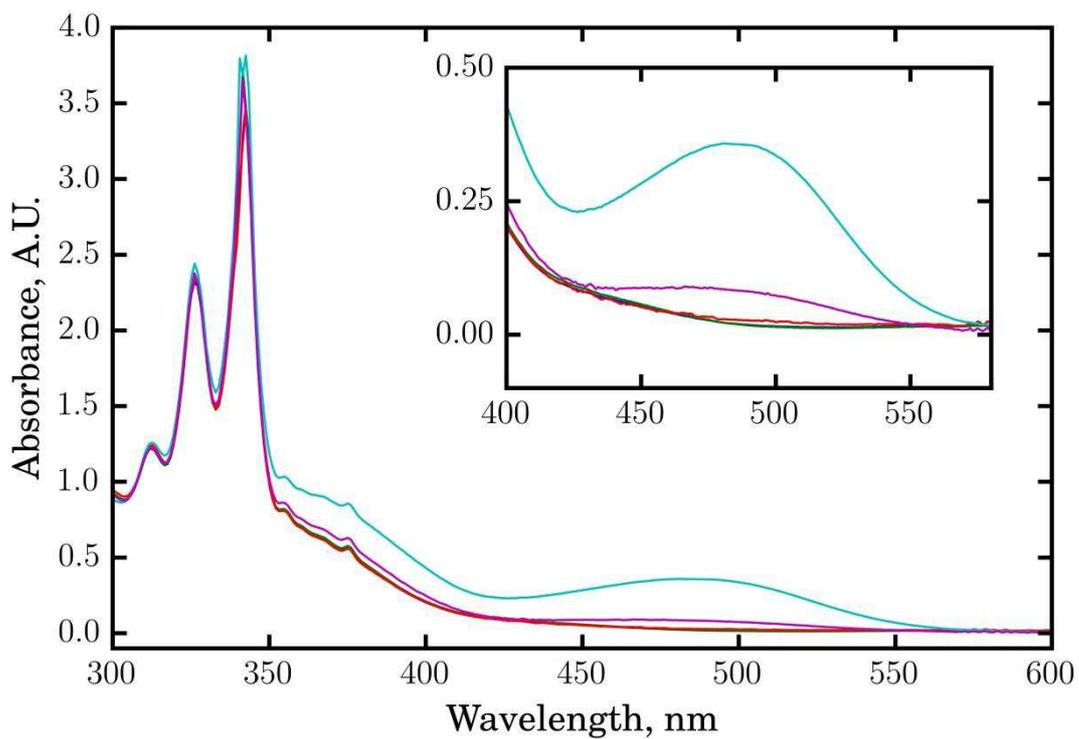
*Figure 5 – Absorbance spectra of **7** (0.1 mM in MeCN): a)[green] **7**; b)[red] **7** after UV irradiation; c)[pink] **7** + Zn(NO₃)₂ (2.5 eq.) after white light irradiation; d)[blue] **7** + Zn(NO₃)₂ (2.5 eq.) after UV irradiation. Inset: Expansion of 400–575 nm region.*
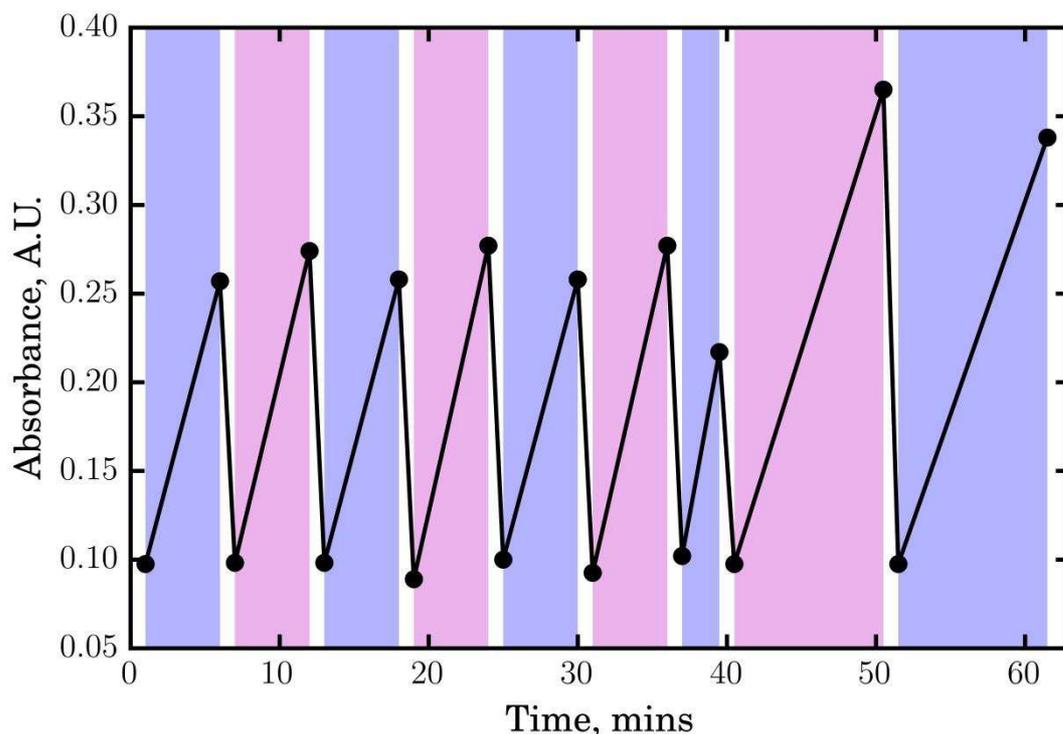
*Figure 6 – Reproducible photochromic behaviour of **7**. Absorbance intensity at 485 nm of a solution of **7** (0.1 mM in MeCN) + Zn(NO₃)₂ (2.5 eq.), exposed to alternating light [white bars], dark [purple bars] and UV [pink bars] cycles.*

Emission spectra were recorded for solutions of 0.1 mM **7** in acetonitrile, exciting both at pyrene (350 nm) and merocyanine (485 nm) wavelengths, and in the absence and presence of Zn^{2+} (Figures 7 and 8). Excitation at 350 nm in the absence of Zn^{2+} resulted in a strong pyrene emission at 400 nm. The intensity of this emission was reduced upon Zn^{2+} addition, with an additional emission peak observed at 620 nm, consistent with merocyanine fluorescence (Figure 7). In this case, the presence of Zn^{2+} promotes merocyanine formation, hence this additional peak is presumably due to merocyanine emission promoted by energy transfer from the pyrene excited state[12] (hence **7** could, in principle, function as a ratiometric fluorescence probe for Zn^{2+} by excitation at 350 nm and then measurement of $I_{620\,nm}/I_{400\,nm}$ as

a function of $[Zn^{2+}]$.)[13] Excitation at 485 nm in the absence of zinc produced no emission; however, in the presence of Zn^{2+} an emission peak at 620 nm was observed (Figure 8).
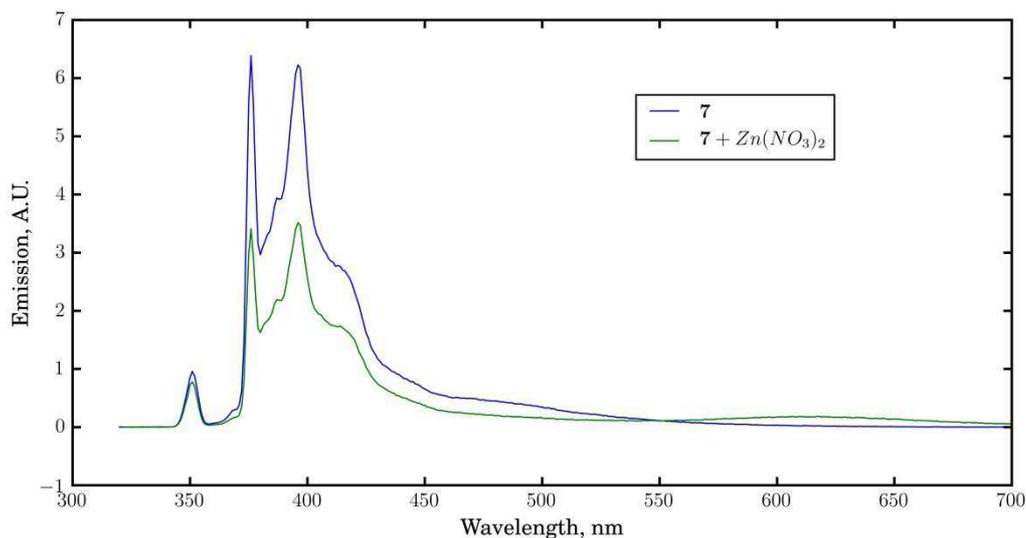
*Figure 7 – Emission spectra (exciting at 350 nm) of: a) **7** (0.1 mM in MeCN; b) **7** (0.1 mM in MeCN) + Zn(NO₃)₂ (2.5 eq.). Each measurement was taken following 15 minutes in the dark.*
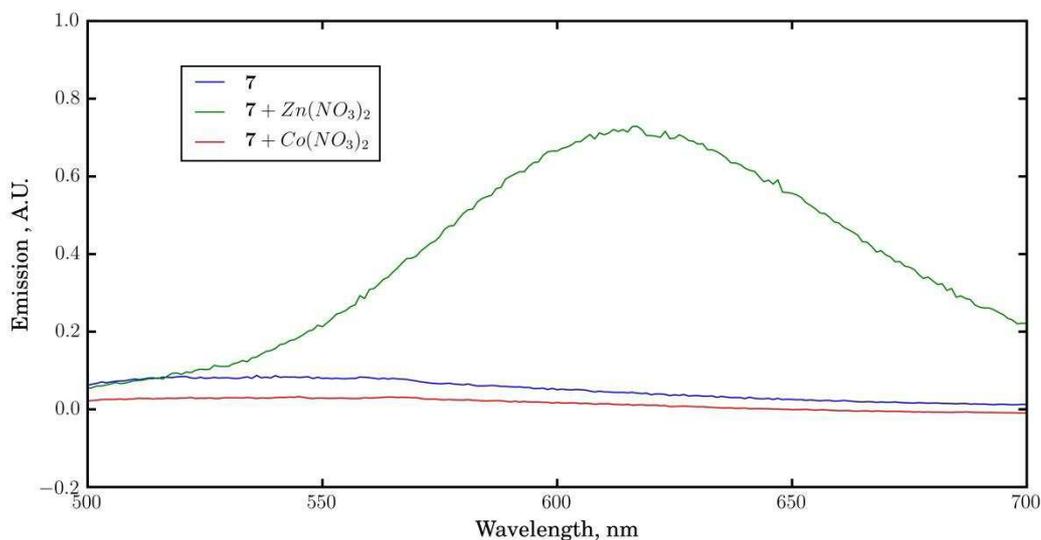
*Figure 8 – Emission spectra (exciting at 485 nm) of: a) **7** (0.1 mM in MeCN; b) **7** (0.1 mM in MeCN) + Zn(NO₃)₂ (2.5 eq.); c) **7** (0.1 mM in MeCN) + Co(NO₃)₂ (2.5 eq.). Each measurement was taken following 15 minutes in the dark.*

12

In addition to Zn^{2+}, 1 mM solutions of **7** in acetonitrile were exposed to a range of potentially competing metal cations and their response was assessed by UV-visible spectroscopy (Figure 9). Of these cations, only Co^{2+} showed any capacity to promote merocyanine formation and, in this case, absorbance at 485 nm was considerably lower than that observed in the presence of Zn^{2+}. Furthermore, an acetonitrile solution of **7** and Co^{2+} produced very limited emission upon excitation at 485 nm, *i.e.* fluorescence spectroscopy provides an effective method to distinguish Co^{2+} and Zn^{2+} in situations where they might be competitive for **7** (Figure 8). This contrast in metal ion selectivity between absorbance and fluorescence measurements has previously been observed in spiropyran-aminoquinolone dyads.[13]
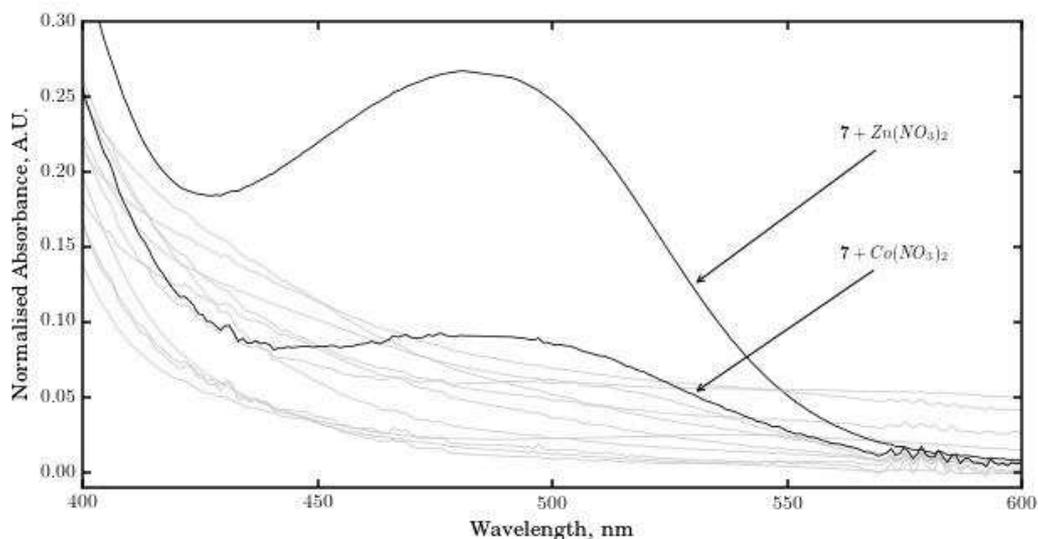
*Figure 9 – Absorbance spectra of **7** (0.1 mM in MeCN) in the presence of various metal salts (2.5 eq.): Zn(NO₃)₂ and Co(NO₃)₂ (highlighted); AgNO₃; Cu(NO₃)₂; Al(NO₃)₃; Mg(NO₃)₂; KNO₃; Cr(NO₃)₃; Ni(NO₃)₂; CaCl₂; NaCl; FeCl₃; Pb(OAc)₂.*

2.2.2. Complex stoichiometry and binding constant of 7 + Zn^{2+}

With the Zn^{2+} selectivity of the spiropyran-pyrene dyad established, we next sought detailed

understanding of the physical parameters of Zn^{2+} chelation. The stoichiometry of the

complex formed between the spiropyran **7** ('Sp') and Zn^{2+} in acetonitrile was determined

from the Job plot shown in Figure 10.[14] This plot is of absorbance, A, at 485 nm (the peak

absorbance wavelength for the complex) as a function of the mole fraction of zinc ion,

$x(Zn^{2+})$, defined in terms of $[Sp]_T$ and $[Zn^{2+}]_T$, the total (bound-plus-unbound) concentrations

of Sp and Zn^{2+}, respectively, as

$$x(Zn^{2+}) = \frac{[Zn^{2+}]_T}{[Sp]_T + [Zn^{2+}]_T} \tag{1}$$

with the value of $[Sp]_T + [Zn^{2+}]_T$ here held constant at 0.2×10^{-3} mol dm^{-3}. The maximum

absorbance occurs at $x(Zn^{2+}) = 0.5$, indicating a ratio of spiropyran to Zn^{2+} of, on average,

1:1. Considering this result and the spiropyran molecular structure, the complex is presumed

to involve a single spiropyran molecule and a single Zn^{2+} ion, and is represented as Sp:Zn^{2+}

in the reaction stoichiometry

$$Sp + Zn^{2+} = Sp:Zn^{2+} \tag{2}$$

The binding constant, K, for this complex formation is defined in terms of $[Sp:Zn^{2+}]$, $[Sp]_u$

and $[Zn^{2+}]_u$, the concentrations of the complex, the unbound spiropyran and the unbound

Zn^{2+}, respectively, as

$$K = \frac{[Sp:Zn^{2+}]}{[Sp]_u[Zn^{2+}]_u} \tag{3}$$

In order to determine the value of K (here at 295 K), the value of $[Sp]_T$ was fixed 0.1×10^{-3}

mol dm^{-3} and absorbance values at 485 nm recorded as a function of $[Zn^{2+}]_T$, as shown

Figure 11. These absorbance values are presumed to be a sum of two Beer-Lambert law

terms as

$$A = \varepsilon_S[Sp]_u l + \varepsilon_{SZ}[Sp:Zn^{2+}]l \tag{4}$$

14

where ε_S and ε_{SZ} are the molar absorption coefficients at 485 nm of the unbound spiropyran and the complex, respectively, and l is the path length of the cell.

Noting the following relation between concentrations

$$[\text{Sp}]_T = [\text{Sp}]_u + [\text{Sp}:\text{Zn}^{2+}] \tag{5}$$

and defining $A_0 = \varepsilon_S [\text{Sp}]_T l$ as the absorbance at $[\text{Zn}^{2+}]_T = 0$, equation (4) is recast as

$$A - A_0 = (\varepsilon_{SZ} - \varepsilon_S)[\text{Sp}:\text{Zn}^{2+}] l \tag{6}$$

Then, in addition to equation (5), the relation between concentrations

$$[\text{Zn}^{2+}]_T = [\text{Zn}^{2+}]_u + [\text{Sp}:\text{Zn}^{2+}] \tag{7}$$

is used to recast equation (3) as

$$K = \frac{[\text{Sp}:\text{Zn}^{2+}]}{([\text{Sp}]_T - [\text{Sp}:\text{Zn}^{2+}])([\text{Zn}^{2+}]_T - [\text{Sp}:\text{Zn}^{2+}])} \tag{8}$$

before rearranging to a quadratic in [Sp:Zn^{2+}] with the physically-reasonable solution

$$[\text{Sp}:\text{Zn}^{2+}] = \frac{1}{2}\left(C_{tot} + \frac{1}{K} - \sqrt{C_{diff}^2 + \frac{2C_{tot}}{K} + \frac{1}{K^2}} \right) \tag{9}$$

where $C_{tot} = [\text{Sp}]_T + [\text{Zn}^{2+}]_T$ and $C_{diff} = [\text{Sp}]_T - [\text{Zn}^{2+}]_T$.

(Written for the limit of large K, the general solution to the quadratic is

$$[\text{Sp}:\text{Zn}^{2+}] = \frac{1}{2}\left(C_{tot} \pm \sqrt{C_{diff}^2} \right)$$

but the positive term in parentheses is rejected since it returns the unreasonable result that [Sp:Zn^{2+}] = [Sp]$_T$ when [Zn^{2+}] = 0.)

Equation (9) was independently-derived but is equivalent to that published by Olson and Bühlmann.[14] As a novel means to extract binding constants from absorbance data, the equation was used to generate values of [Sp:Zn^{2+}] with simple trial-and-error variation of K until, in accord with equation (6) and judged by linear regression analysis using the standard r^2 value, the greatest degree of linearity was achieved in a plot of [Sp:Zn^{2+}] as a function of A

15

$- A_0$. The greatest degree of linearity ($r^2 = 0.9947$) was achieved using a value of $K = 1.4 \times 10^4 \, mol^{-1} \, dm^3$ and the corresponding plot of [Sp:Zn^{2+}] as a function of $A - A_0$ is shown in Figure 12. This value of K at 295 K is reasonable, relative to that of $1.6 \times 10^4 \, mol^{-1} \, dm^3$ at 293 K reported by Natali et al.[10] for the analogous zinc-binding spiropyran lacking the pyrene unit.
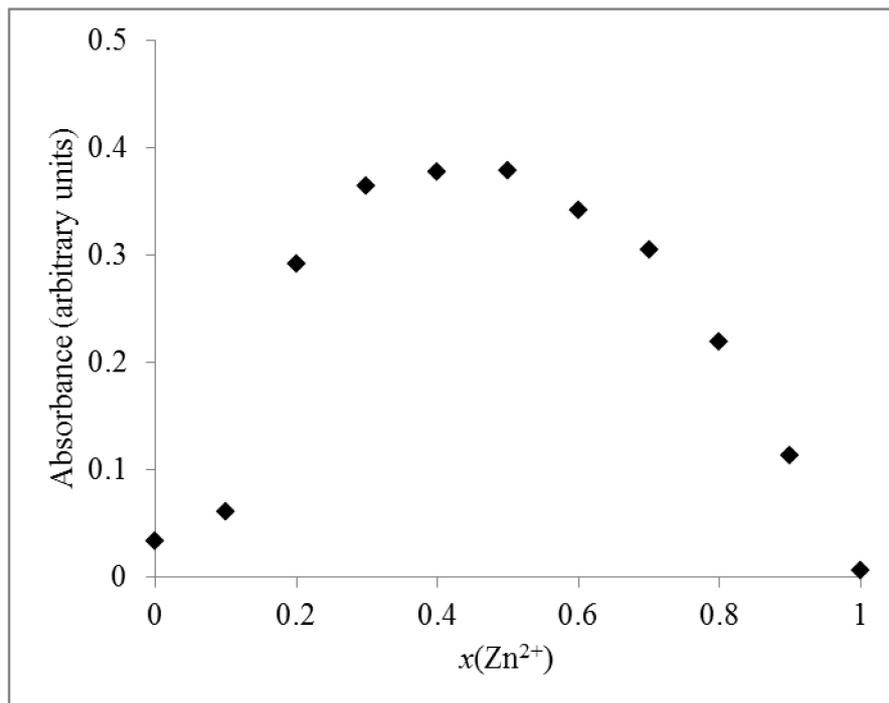
Figure 10 – Job plot of absorbance at 485 nm as a function of the mole fraction of zinc ion, x(Zn^{2+}), for a solution of constant total spiropyran plus zinc ion concentration of 0.2 × 10^{-3} mol dm^{-3} in acetonitrile at 295 K.
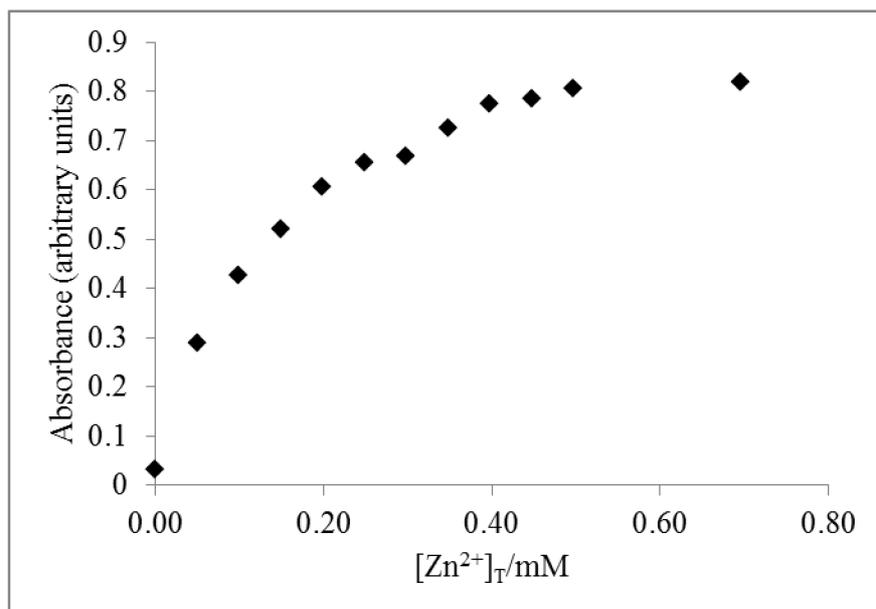
Figure 11 – Absorbance at 485 nm as a function of the total (bound-plus-unbound) zinc ion concentration, $[Zn^{2+}]_T$, of a solution also containing 0.1×10^{-3} mol dm^{-3} spiropyran in acetonitrile at 295 K.
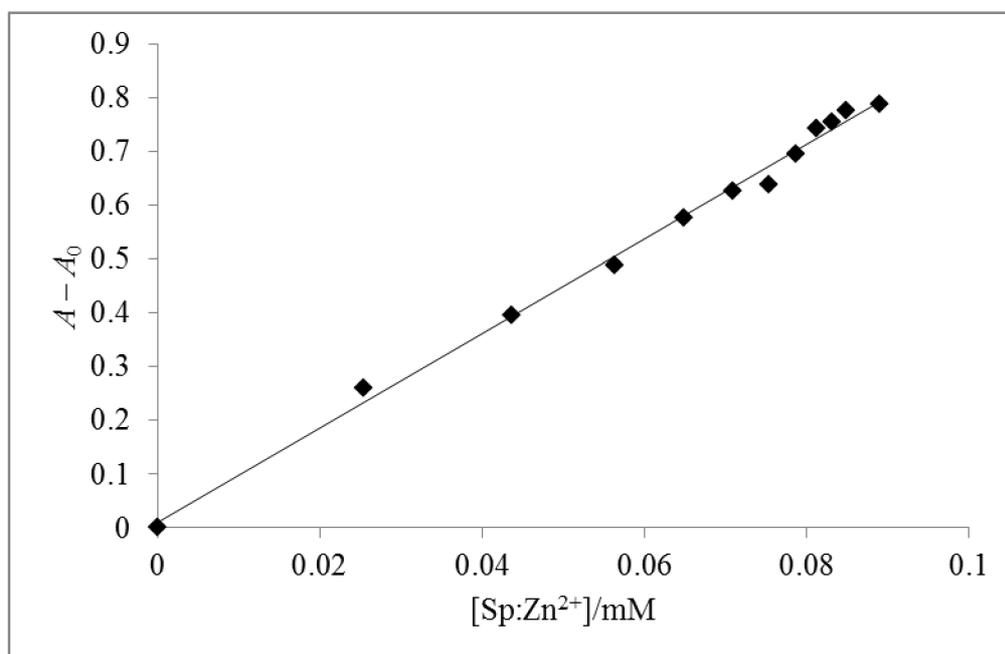
Figure 12 – Linear plot ($r^2 = 0.9947$) of $A - A_0$ (A is the absorbance in arbitrary units, with A_0 denoting its value in the absence of Zn^{2+}) at 485 nm as a function of the complex concentration, $[Sp:Zn^{2+}]$, calculated using equation (9) with a value of binding constant of $K = 1.4 \times 10^4$ mol^{-1} dm^3 in acetonitrile at 295 K.

Also apparent from the data presented in Figure 11 is the upper limit of the [**7**]:[Zn^{2+}] ratio that **7** can tolerate as an effective sensor for Zn^{2+}. Maximum binding for **7** with $Zn(NO_3)_2$ in acetonitrile required ~5 eq. of the zinc salt; any further increase in [Zn^{2+}] did not result in an increase in [**7-**MC]. Consequently, **7** can function as an effective sensor for [Zn^{2+}] up to a point where [Zn^{2+}] is in five-fold excess.

In general, the solution behaviour of **7** towards Zn^{2+} (selectivity, binding stoichiometry, binding constant and photochromism) closely followed that of the parent compound **6** (Figure 2) lacking the pyrene moiety. Detailed analysis of the **6**–Zn^{2+} complex by Natali et al.[10] identified tridentate Zn^{2+} coordination through phenolate, methoxy and pyridine groups (see Figure 3); we assume that a similar binding model for **7**–Zn^{2+} is appropriate. In any case, that the Zn^{2+} binding properties of **6** and **7** are similar, despite the inclusion of a pyrene group in the latter, gave us incentive to use **7** to derivatise carbon surfaces.

2.3. Hybrid materials: non-covalent functionalisation of graphene oxide, graphene and carbon nanotubes with 7

2.3.1. Synthesis of 7-GO, 7-G and 7-CNT

Having assessed its solution behaviour, the non-covalent functionalisation of graphene oxide, graphene and CNTs using **7** was examined. The addition of **7** to a dispersion of each carbon-based material in acetonitrile (see experimental section) was followed, after 1 hour, by analysis using UV-vis and fluorescence spectroscopy (Figure 13). In each case, absorbance at 340 nm confirmed the presence of **7**, but excitation at 340 nm resulted in sufficiently little emission to indicate quenching of pyrene fluorescence and so the adsorption of pyrene on the carbon surface. Non-covalent interactions of pyrene and carbon surfaces allow efficient

energy transfer from – and hence quenching of – pyrene excited states and therefore

fluorescence quenching indicates that such pyrene–carbon interactions have formed.[4a]
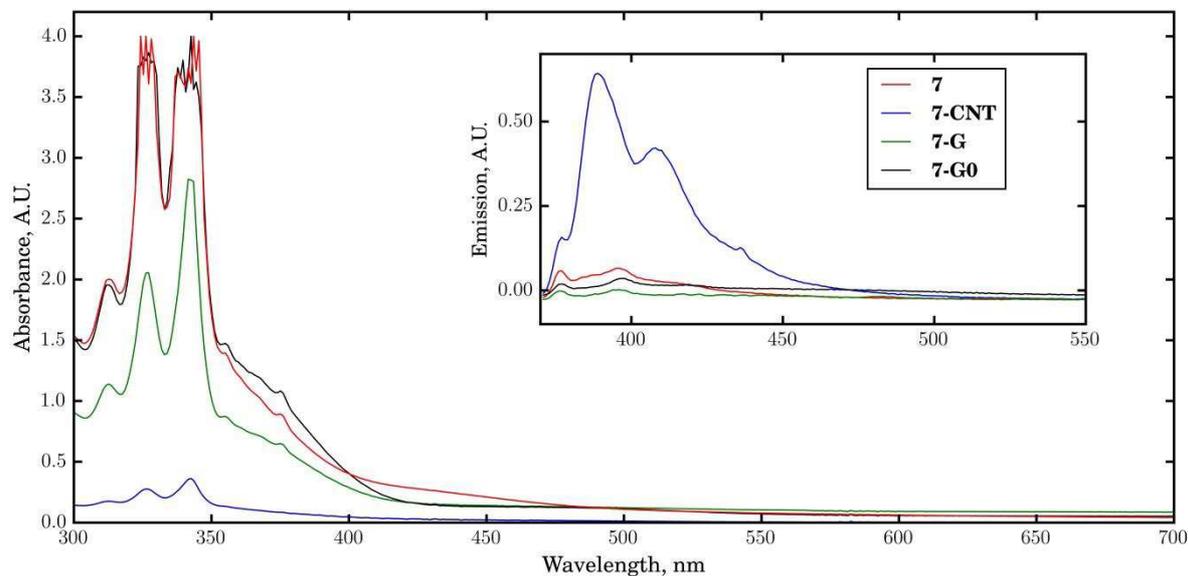
*Figure 13 – Absorbance and (inset) emission spectra of **7** and **7** adsorbed onto CNTs,*

graphene and graphene oxide. Pyrene absorbance is retained in the hybrid materials,

whereas pyrene fluorescence is quenched.

2.3.2. Zn^{2+} binding properties of 7-GO, 7-G and 7-CNT

The Zn^{2+} binding behaviour of each novel hybrid material was examined: dispersions of **7**-

GO, **7**-G and **7**-CNT in acetonitrile were exposed to zinc(II) nitrate, then kept in darkness for

5 minutes. Both graphene- and carbon nanotube-supported **7** showed strong absorbance at

485 nm, consistent with merocyanine formation and concomitant Zn^{2+} binding, and

confirmed that the solution behaviour of **7** could be preserved whilst non-covalently bound to

a carbon surface (Figure 14). Moreover, **7**-G and **7**-CNT displayed similar photochromic

behaviour to free **7**, with exposure to alternate dark / light cycles triggering Zn^{2+} binding and

release respectively. In contrast, **7**-GO did not display any evidence of merocyanine

formation upon exposure to zinc(II) nitrate, regardless of darkness or light irradiation, even

19

with addition of excess Zn^{2+}. Furthermore, addition of dispersed GO in acetonitrile to a solution of Zn^{2+}-bound MC-**7** in darkness resulted in rapid decolouration and irreversible loss of merocyanine absorbance. We assume that the oxygen-based functionality displayed by GO (and not present in either graphene or CNTs) can disrupt the precise Zn^{2+} binding site offered by MC-**7**, thus rendering the merocyanine form inaccessible. Although GO is able to adsorb metal cations such as Zn^{2+},[15] the idea that GO is competing with the spiropyran for Zn^{2+} can be discounted because the merocyanine form is not observed when **7**-GO is exposed to a sufficiently large excess of Zn^{2+} such that free binding sites on the GO are likely to be saturated.
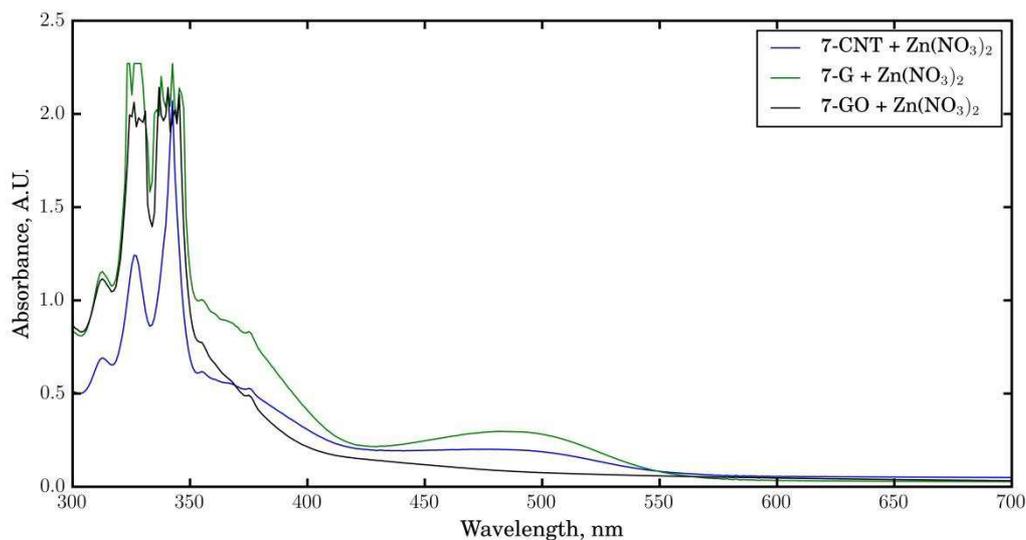
*Figure 14 – Absorbance spectra of hybrid materials **7**-GO, **7**-CNT and **7**-G in the presence of Zn(NO₃)₂ after 5 minutes of darkness.*

3. Conclusion

We have developed a spiropyran-based cation receptor capable of non-covalent functionalization of carbon surfaces. Cation binding occurs with concomitant isomerisation of the spiropyran to a highly-coloured merocyanine form; hence bound cation concentration can be estimated by simple absorbance or emission spectroscopy. The receptor shows high selectivity and sensitivity towards Zn^{2+} over other potentially competitive species. Analysis of Zn^{2+} binding in acetonitrile shows 1:1 binding stoichiometry with a binding constant of 1.4 $\times 10^4$ mol^{-1} dm^3. The merocyanine-Zn^{2+} complex is light sensitive and irradiation with white light promotes photoisomerisation to the spiropyran form with release of Zn^{2+}. Return to dark conditions, or UV irradiation, promotes merocyanine formation and Zn^{2+} uptake. This photochromic behaviour is reproducible over many light-dark cycles.

The design of the receptor incorporates a pyrene unit. In solution, the pyrene can serve as a reference chromophore to quantify changes in merocyanine absorbance or emission, hence invites possible use of **7** as a ratiometric probe for Zn^{2+}. Furthermore, the pyrene moiety provides a versatile anchor group for facile non-covalent attachment of the spiropyran receptor to carbon-based materials. Accordingly, we have synthesised hybrid spiropyran-carbon materials based upon carbon nanotubes, graphene and graphene oxide. Although spiropyran adsorption was successful in all cases, spiropyran bound to graphene oxide did not undergo isomerisation to its merocyanine form upon exposure to Zn^{2+}. Conversely, hybrid spiropyran-graphene and spiropyran-CNT exhibited spiropyran-merocyanine photoisomerism in the presence of Zn^{2+}. To our knowledge, these materials constitute the first examples of spiropyran-based cation receptors non-covalently attached to carbon surfaces. Investigation into the spectroelectronic properties of these novel dynamic materials is ongoing.

21

4. Experimental

4.1. General experimental

All chemicals were purchased from Aldrich and were used as received. The fraction of light petroleum ether boiling in the range 40 to 60 °C is referred to as "petrol". ^{1}H NMR spectra were recorded at 300 MHz using a Bruker ACF300 spectrometer. Chemical shifts are quoted in ppm relative to tetramethylsilane, the residual solvent peak being used for referencing purposes where possible. Coupling constants are quoted to the nearest 0.5 Hz with peak multiplicities for single resonances being labelled as: s, singlet; d, doublet; t, triplet; q, quartet; m, unresolved multiplet. ^{13}C NMR spectra were recorded on the same instrument at 75 MHz. Analytical thin layer chromatography was carried out using Merck Kieselgel 60 F254, coated on aluminium plates, with visualisation of spots where necessary by quenching of UV(254 nm) fluorescence or by staining with $KMnO_4$. Silica gel with particle size 40−63 mm was used for flash chromatography. A Büchi R110 Rotovapor was used for the removal of solvents under reduced pressure, with a water or dry ice condenser being used as appropriate. Mass spectra were obtained by the EPSRC National Mass Spectrometry Facility, Swansea, UK using positive ion electrospray ionisation (labelled as ES). Infrared spectra were recorded using a NicoletMagna 550 spectrometer. Generally, only major absorbances are quoted. Thin film samples were produced by evaporation of a dilute chloroform or dichloromethane solution of the sample on a sodium chloride plate. UV-Visible absorption measurements were recorded on a Thermo Scientific Evolution Array UV-Visible Spectrophotometer, scanning from 190 - 1100 nm and using quartz cuvettes of 1 cm path length.

4.2. Synthesis

2-Bromomethyl-6-(4-((1-pyrenyl)butoxy)methyl)pyridine 10

Anhydrous THF (16 mL) was slowly added, with stirring, to sodium hydride (30 mg of a 60% dispersion in mineral oil, 0.755 mmol, 2 eq.) at 0 °C under N_2. To the resulting suspension was added 1-pyrenebutanol (104 mg, 0.379 mmol, 1 eq.) then 2,6-bis(bromomethyl)pyridine (200 mg, 0.755 mmol, 2 eq.) and the reaction was heated to reflux. After 18 h, the reaction was cooled to 0 °C and water (15 mL) was slowly added. The reaction was extracted with ethyl acetate (3 × 15 mL), and the combined organic fractions were dried ($MgSO_4$) and concentrated *in vacuo*. The resulting crude product was purified by flash chromatography, eluting with 1:9 then 2:8 ethyl acetate:petrol, to give the *pyridine* **10** (108 mg, 62%) as a colourless oil, R_f 0.4 (2:8 ethyl acetate:petrol); v_{max}/cm^{-1}: 3040, 2936, 2862, 1591, 1456, 1121 and 846; ^{1}H NMR (300 MHz, $CDCl_3$): δ = 8.30 (1 H, d, J = 9.0 Hz, pyrene 8-H), 8.20-7.95 (7 H, m, pyrene 3-7, 9,10-H), 7.89 (1 H, d, J = 8.0 Hz, pyrene 2-H), 7.63 (1 H, t, J = 7.5 Hz, pyridine 4-H), 7.36 (1 H, d, J = 7.5 Hz, pyridine 5-H), 7.30 (1 H, d, J = 7.5 Hz, pyridine 3-H), 4.61 (2 H, s, $ArCH_2O$), 4.50 (2 H, s, CH_2Br), 3.66 (2 H, t, J = 6.5 Hz, CH_2CH_2O), 3.39 (2 H, t, J = 7.5 Hz, pyreneCH_2), 2.10-1.93 (2 H, m, CH_2CH_2O) and 1.93-1.78 (2 H, m, pyreneCH_2CH_2); ^{13}C NMR (75 MHz, $CDCl_3$): δ = 158.9, 156.0, 137.7, 136.8, 131.5, 130.9, 129.8, 128.6, 127.5, 127.3, 127.2, 126.6, 125.3, 125.11, 125.05, 124.9, 124.8, 124.7, 123.5, 122.1, 120.5, 73.5, 71.0, 33.8, 33.3, 29.8 and 28.4; HRMS-ES (*m/z*): Found: 458.1106 (MH^+, $C_{27}H_{25}ONBr$ requires: 458.1114).

1-(6-(4-((1-pyrenyl)butoxy)methyl)pyridin-2-yl)methyl-3,3-dimethyl-2-methylidene-2,3-dihydro-1*H*-indole 12

2,3,3-Trimethylindolenine (49 μL, 0.303 mmol, 1.7 eq.) was added to a stirred suspension of the pyridine **10** (82 mg, 0.179 mmol, 1 eq.) and potassium carbonate (99 mg, 0.714 mmol, 8

eq.) in acetonitrile (8 mL) under N_2. The reaction was heated to reflux for 40 h and then partitioned between water (10 mL) and dichloromethane (10 mL). The aqueous phase was extracted with dichloromethane (3 × 10 mL) and the combined organic fractions were dried (MgSO$_4$) and concentrated *in vacuo*. The resulting crude *indole* **12** was used directly in the following step. ^{1}H NMR (300 MHz, CDCl$_3$): δ = 8.17 (1 H, d, *J* = 9.0 Hz, pyrene 8-H), 8.08-7.85 (7 H, m, pyrene 3-7, 9,10-H), 7.77 (1 H, d, *J* = 8.0 Hz, pyrene 2-H), 7.45 (1 H, t, *J* = 7.5 Hz, pyridine 4-H), 7.27-7.05 (2 H, m, pyridine 3 and 5-H), 6.96 (1 H, t, *J* = 7.5 Hz, indole 6-H), 6.80 (1 H, d, *J* = 7.5 Hz, indole 4-H), 6.70 (1 H, t, *J* = 7.5 Hz, indole 5-H), 6.39 (1 H, d, *J* = 7.5 Hz, indole 7-H), 4.72 (2 H, s, ArCH$_2$O), 4.55 (2 H, s, CH$_2$N), 3.78 (2 H, s, =CH$_2$), 3.60-3.46 (2 H, m, CH$_2$C*H$_2$*O), 3.34-3.22 (2 H, m, pyreneCH$_2$), 1.98-1.65 (4 H, m, C*H$_2$*C*H$_2$*O), 1.32 (3 H, s, Me) and 1.20 (3 H, s, Me).

8-Methoxy-3′,3′-dimethyl-6-nitro-1′-((6-(4-((1-pyrenyl)butoxy)methyl)pyridin-2-yl)methyl)-spiro(chromene-2,2′-indoline) 7

3-Methoxy-5-nitrosalicylaldehyde (35 mg, 0.179 mmol) was added to a stirred solution of the crude indole **12** in ethanol–dichloromethane (4:1, 5 mL) and the reaction was stirred at 55 °C. After 20 h, the reaction was concentrated *in vacuo* and the resulting crude product was purified by flash column chromatography, eluting with 25:75 ethyl acetate:petrol, to give the *spiropyran* **7** (23 mg, 18% from **10**) as a green oil, R_f 0.2 (2:8 ethyl acetate:petrol); ν$_{max}$/cm^{-1}: 2922, 2850, 1718, 1459, 1335, 1270, 1090 and 848; ^{1}H NMR (300 MHz, CDCl$_3$): δ = 8.19 (1 H, d, *J* = 9.0 Hz, pyrene 8-H), 8.10-7.86 (7 H, m, pyrene 3-7, 9,10-H), 7.78 (1 H, d, *J* = 8.0 Hz, pyrene 2-H), 7.54 (1 H, d, *J* = 2.5 Hz, chromene 5-H), 7.48 (1 H, d, *J* = 2.5 Hz, chromene 7-H), 7.48 (1 H, t, *J* = 8.0 Hz, pyridine 4-H), 7.19 (1 H, d, *J* = 8.0 Hz, pyridine 3-H), 7.14 (1 H, d, *J* = 8.0 Hz, pyridine 5-H), 7.04 (1 H, d, *J* = 7.5 Hz, indoline 4-H), 6.97 (1 H, t, *J* = 7.5 Hz, indoline 6-H), 6.78 (1 H, t, *J* = 7.5 Hz, indoline 5-H), 6.70 (1 H, d, *J* = 10.5 Hz,

chromene 4-H), 6.20 (1 H, d, J = 7.5 Hz, indoline 7-H), 5.77 (1 H, d, J = 10.5 Hz, chromene 3-H), 4.52 (1 H, d, J = 10.0 Hz, CH$_2$N), 4.51 (2 H, s, ArCH$_2$O), 4.25 (1 H, d, J = 10.0 Hz, CH$_2$N), 3.64 (3 H, s, OMe), 3.54 (2 H, t, J = 6.5, CH$_2$CH_2O), 3.30 (2 H, t, J = 7.5 Hz, pyreneCH$_2$), 1.92-1.81 (2 H, s, CH_2CH$_2$O), 1.80-1.68 (2 H, m, pyreneCH$_2$CH_2), 1.26 (3 H, s, Me) and 1.18 (3 H, s, Me); ^{13}C NMR (75 MHz, CDCl$_3$): δ = 158.1, 157.6, 148.8, 147.3, 146.4, 140.4, 137.7, 136.7, 136.1, 131.4, 130.9, 129.8, 128.7, 128.6, 127.6, 127.5, 127.3, 127.2, 126.6, 125.8, 125.1, 125.0, 124.84, 124.79, 124.7, 124.6, 123.4, 121.8, 121.0, 119.9, 119.8, 118.1, 115.3, 107.9, 107.6, 106.0, 73.3, 71.1, 60.4, 56.2, 52.5, 33.3, 30.2, 28.4, 20.0 and 14.2; HRMS-ES (*m/z*): Found: 716.3116 (MH$^+$, C$_{46}$H$_{42}$O$_5$N$_3$ requires: 716.3119).

7-Graphene Hybrid (7-G)

Graphite (20 mg) was added to acetonitrile (5 mL) and the resulting suspension was sonicated for 18 h then centrifuged (10000 rpm, 10 mins).[16] 2.5 mL of supernatant was isolated from aggregated material, and spiropyran **7** (150 µL of a 6 mg/mL solution in acetonitrile; 0.9 mg, 0.00126 mmol) was added and stirred for 1 h to give the **7**-graphene hybrid dispersed in acetonitrile.

7-Carbon nanotube hybrid (7-CNT)

Carbon nanotubes (0.5 mg) were added to acetonitrile (3 mL) and sonicated for 5 minutes then allowed to settle for 10 minutes.[4] 2.5 mL of supernatant was isolated from aggregated material, and spiropyran **7** (150 µL of a 6 mg/mL solution in acetonitrile; 0.9 mg, 0.00126 mmol) was added and stirred for 1 h to give the **7**-CNT hybrid dispersed in acetonitrile.

7-GO hybrid (7-GO)

25

Graphene oxide flakes (5 mg) were added to acetonitrile (5 mL) and the resulting suspension was sonicated for 4 h then centrifuged (10000 rpm, 10 mins).[17] 2.5 mL of supernatant was isolated from aggregated material, and spiropyran **7** (150 µL of a 6 mg/mL solution in acetonitrile; 0.9 mg, 0.00126 mmol) was added and stirred for 1 h to give the **7**-GO hybrid dispersed in acetonitrile.

4.3. Binding Studies of 7

4.3.1 Comparison of binding of 7 to various metal cations

ML_n (5 µL of 0.1 M solution in water, 0.5 µmol, 2.5 eq.) was added to **7** (2 mL of a 0.1 mM solution in acetonitrile, 0.2 µmol, 1 eq.). The resulting solution was shaken, irradiated with white light for 1 minute, placed in darkness for 5 minutes then analysed by UV-visible and fluorescence spectroscopy.

4.3.2. Determination of maximum binding of 7 with $Zn(NO_3)_2$ in acetonitrile

Aliquots containing **7** (0.2 µmol, 1 eq.) and $Zn(NO_3)_2.5H_2O$ (0 − 1.4 µmol, 0 − 7 eq.) in acetonitrile (2.01 mL) were placed in darkness for 20 h, then analysed by UV-visible spectroscopy.

4.3.3. Determination of 7-Zn^{2+} binding stoichiometry by Job Plot analysis

11 aliquots were prepared, each containing a total of 0.0004 mmol of $Zn(NO_3)_2.5H_2O$ + **xx** in acetonitrile (2.004 mL), such that $[Zn^{2+}]$ / ($[Zn^{2+}]$ + [**7**]) varied from 0 to 1.0, in 0.1 increments. Each aliquot was placed in darkness for 20 h, then analysed by UV-visible spectroscopy.

26

5. Acknowledgements

6. References

1. Fischer, E.; Hirshberg, Y. *J. Chem. Soc.* **1952,** 4522–4524.

2. Klajn, R.; *Chem. Soc. Rev.* **2014,** *43,* 148–184.

3. Del Canto, E.; Flavin, K.; Natali, M.; Perova, T.; Giordani, S. *Carbon* **2010,** *48,* 2815–2824.

4. a. Setaro, A.; Bluemmel, P.; Maity, C.; Hecht, S.; Reich, S. *Adv. Funct. Mater.* **2012,** *22,* 2425–2431.

b. Bluemmel, P.; Setaro, A.; Maity, C.; Hecht, S.; Reich, S. *Phys. Status Solidi B* **2012,** *249,* 2479–2482.

c. Bluemmel, P.; Setaro, A.; Maity, C.; Hecht, S.; Reich, S. *J. Phys.: Condens. Matter* **2012,** *24,* 394005.

5. a. Jang, A.; Jeon, E. K.; Kang, D.; Kim, G.; Kim, B.; Kang, D. J.; Shin, H. S. *ACS Nano* **2012,** *6,* 9207–9213.

b. Joo, P.; Kim, B. J.; Jeon, E. K.; Cho, J. H.; Kim, B. *Chem. Commun.* **2012,** *48,* 10978–10980.

6. a. Malic, E.; Weber, C.; Richter, M.; Atalla, V.; Klamroth, T.; Saalfrank, P.; Reich, S.; Knorr, A. *Phys. Rev. Lett.* **2011,** *106,* 097401.

b. Malic, E.; Setaro, A.; Bluemmel, P.; Sanz-Navarro, C. F.; Ordejón, P.; Reich, S.; Knorr, A. *J. Phys.: Condens. Matter* **2012,** *24,* 394006.

7. a. Bode, N.; Mariani, E.; von Oppen, F. *J. Phys.: Condens. Matter* **2012,** *24,* 394017.

b. Berghäuser, G.; Malic, E. *Phys. Status Solidi B* **2013,** *250,* 2678–2680.

8. Del Canto, E.; Natali, M.; Movia, D.; Giordani, S. *Phys. Chem. Chem. Phys.* **2012,** *14,* 6034–6043.

9. Natali, M.; Aakeröy, C.; Desper, J.; Giordani, S. *Dalton Trans.* **2010,** *39,* 8269–8277.

10. Natali, M.; Soldi, L.; Giordani, S. *Tetrahedron* **2010,** *66,* 7612–7617.

11. Li, Y.; Duan, Y.; Zheng, J.; Li, J.; Zhao, W.; Yang, S.; Yang, R. *Anal. Chem.* **2013,** *85,* 11456–11463.

12. Guo, X.; Zhang, D.; Wang, T.; Zhu, D. *Chem. Commun.* **2003,** *7,* 914–915.

13. Zhu, J. F.; Yuan, H.; Chan, W. H.; Lee, A. W. M. *Tetrahedron Lett.* **2010,** *51,* 3550–3554.

14. a. Olson, E. J.; Bühlmann, P. *J. Org Chem.* **2011,** *76,* 8406–8412.

b. Olson, E. J.; Bühlmann, P. *J. Org Chem.* **2014,** *79,* 830–830.

15. Sitko, R.; Turek, E.; Zawisza, B.; Malicka, E.; Talik, E.; Heimann, J.; Gagor, A.; Feist, B.; Wrzalik, R. *Dalton Trans.* **2013,** *42,* 5682–5689.

16. Du, W.; Jiang, X.; Zhu, L. *J. Mater. Chem. A* **2013,** *1,* 10592–10606.

17. Paredes, J. I.; Villar-Rodil, S.; Martínez-Alonso, A.; Tascón, J. M. D. *Langmuir* **2008,** *24,* 10560–10564.